Experimental Neurology 311 (2019) 225–233

Contents lists available at ScienceDirect

Experimental Neurology

journal homepage: www.elsevier.com/locate/yexnr

Research paper

Astrocyte-specific deletion of Kir6.1/K-ATP channel aggravates cerebral ischemia/reperfusion injury through endoplasmic reticulum stress in mice

Chong-Jin Zhong[a], Miao-Miao Chen[a], Ming Lu[a], Jian-Hua Ding[a], Ren-Hong Du[a,*], Gang Hu[a,b,*]

[a] Jiangsu Key Laboratory of Neurodegeneration, Department of Pharmacology, Nanjing Medical University, 101 Nongmian Avenue, Nanjing, Jiangsu 211166, PR China
[b] Department of Pharmacology, Nanjing University of Chinese Medicine, 138 Xianlin, PR China

ARTICLE INFO

Keywords:
ATP-sensitive potassium channels
Kir6.1
Astrocytes
Cerebral ischemia
Endoplasmic reticulum stress
Apoptosis

ABSTRACT

ATP-sensitive potassium (K-ATP) channels, coupling cell metabolism to cell membrane potential, are involved in brain diseases including stroke. Emerging evidence shows that astrocytes play important roles in the pathophysiology of cerebral ischemia. Kir6.1, a pore-forming subunit of K-ATP channel, is prominently expressed in astrocytes and participates in regulating its function. However, the exact role of astrocytic Kir6.1-containg K-ATP channel (Kir6.1/K-ATP) in ischemic stroke remains unclear. Here, we found that astrocytic Kir6.1 knockout (KO) mice exhibited larger infarct areas and more severe brain edema and neurological deficits in middle cerebral artery occlusion stroke model. Both activated gliosis and neuronal loss were aggravated in astrocytic Kir6.1 KO mice. Furthermore, the protein levels of pro-apoptotic protein Bcl-2 associated X (Bax) and active caspase-3 were up-regulated and the expression of anti-apoptotic protein Bcl-2 was down-regulated in astrocytic Kir6.1 KO mice. This is accompanied by enhanced endoplasmic reticulum stress (ER stress) responses in brain tissues and in astrocytes during ischemia/reperfusion (I/R) injury. Finally, inhibition of ER stress rescued astrocyte apoptosis induced by Kir6.1 deletion during I/R injury. Collectively, our findings reveal that astrocytic Kir6.1/K-ATP channel protects brain from cerebral ischemia/reperfusion injury through inhibiting ER stress and suggest that astrocytic Kir6.1/K-ATP channel is a promising therapeutic target for ischemic stroke.

1. Introduction

Stroke is a central nervous system disease with the highest mortality and disability rates, which causes serious damage to human health (Maier et al., 2017). There are very few effectual treatments for stroke (Zhou et al., 2018). Currently, the only FDA approved treatment is to provide tissue plasminogen activator to reopen occluded blood vessels (Moussaddy et al., 2018). However, this treatment is only appropriate for a very small number of patients due to a narrow time window and complications (You et al., 2018). Unfortunately, almost all clinical studies to find new drugs with neuroprotective effects for stroke fail in recent years (Ginsberg, 2008). Therefore, the development of new stroke therapy strategies is especially urgent for stroke patients. Studies have shown that the protection of neurological function should not be limited to the protection of single neuron and may pay more attention to astrocytes (Koizumi et al., 2018).

Astrocytes are the most abundant cells in the central nervous system (CNS) and express a wide range of channels, neurotransmitter receptors, and transporters. Although these molecules control neuronal functions under physiological conditions, they also play important roles in regulation of pathological brain functions such as ischemic (Hirayama et al., 2015). Accumulating evidence suggests that glial cells have various roles in regulating brain functions, including modulation of synaptic transmission, neuronal excitation, and neuronal structure. In addition, astrocytes are closely related to homeostasis, stability of brain function, and protection of neurons (Khakh and Sofroniew, 2015). More recently, based on transcriptome analysis, reactive astrocytes are characterized into two types: neurotoxic A1 and protective A2 (Liddelow et al., 2017). A2-like astrocytes release gliotransmitters such as ATP and glutamate, neurotrophic factors and erythropoietin to protect the neurons in ischemia. In contrast, A1-like astrocytes produce excitatory amino acids and inflammatory factors to damage the neurons (Clarke et al., 2018; Yun et al., 2018). Thus, astrocytes play a crucial role in the progression of stroke and it is important to determine the role and mechanism of astrocytes, which may provide new targets for the treatment of ischemic stroke.

ATP-sensitive potassium (K-ATP) channels are the unique channels coupling cell metabolism to cell membrane potential (Rubaiy, 2016).

* Corresponding authors at: Jiangsu Key Laboratory of Neurodegeneration, Department of Pharmacology, Nanjing Medical University, 101 Nongmian Avenue, Nanjing, Jiangsu 211166, PR China.
E-mail addresses: drh@njmu.edu.cn (R.-H. Du), neuropha@njmu.edu.cn (G. Hu).

https://doi.org/10.1016/j.expneurol.2018.10.005
Received 4 July 2018; Received in revised form 27 September 2018; Accepted 9 October 2018
Available online 10 October 2018
0014-4886/

They are hetero-octamers composed of pore-forming Kir6.x (6.1 or 6.2) subunits and sulfonylurea receptor (SUR1 or SUR2) regulatory subunits, regulated by intracellular ATP and ADP concentrations. K-ATP channels are involved in many brain diseases including stroke (Du et al., 2018; Dong et al., 2013). As a metabolic sensor, K-ATP channels are widely expressed in most metabolically active tissues, including brain, heart and pancreatic β-cells (Tinker et al., 2014). Within the brain, Kir6.2 is predominantly expressed in neurons and Kir6.2 knockout aggravates the neuron death after ischemic insults (Sun and Feng, 2013). Kir6.1 is mainly expressed in astrocytes (Thomzig et al., 2001) and microglia (Zhou et al., 2008). Our previous study showed that opening of K-ATP channels could alleviate ischemia-induced neuroinflammation (Dong et al., 2016). Nevertheless, the role of astrocytic Kir6.1-containing K-ATP (Kir6.1/KATP) channel in ischemia stroke remains unknown. In the present study, we prepared middle cerebral artery occlusion (MCAO) model with astrocytic Kir6.1 knockout mice to investigate the role of astrocytic Kir6.1/KATP channel in ischemic stroke.

2. Materials and methods

2.1. Experimental animals

Astrocyte-specific Kir6.1 knockout mice ($Kir6.1^{loxp/loxp}$ $GFAP^{Cre}$) were generated by breeding the Kir6.1 floxed mice (obtained from Model Animal Resource Center, Nanjing, China) with GFAP-driven Cre recombinase mice (obtained from Jiawei Zhou's laboratory). $Kir6.1^{loxp/loxp}$ (WT) littermates were used as controls. Genotyping of the mice was performed using sequence-specific primers Kir6.1-floxp and Cre (Fig. S1). Mice (C57Bl/6 background) were bred and maintained in the Animal Resource Centre of the Faculty of Medicine, Nanjing Medical University. Mice had free access to food and water in a room with an ambient temperature of 22 °C ± 2 °C and a 12: 12-h light/dark cycle. All animal procedures were performed in strict accordance with the guideline of the Institutional Animal Care and Use Committee of Nanjing Medical University.

2.2. Middle cerebral artery occlusion (MCAO) model

Mice (male, 12–16 weeks) were anesthetized with an intraperitoneal injection of chloral hydrate (3.5 mg/kg). The modified mono-filament intraluminal MCAO procedure was used in our experiments. The rectal temperature was maintained at 37 °C ± 0.2 °C using a heating pad and a heating lamp throughout the entire procedure. 6–0 silicone-coated nylon monofilament (6023PK, Doccol Corp, CA, USA) was delivered to the right internal carotid artery via the external carotid artery and the right common carotid artery was temporarily ligated. Laser-Doppler flowmetry (Moor VSM-LDF, wilmington, DE, USA) was used to monitor regional cerebral blood flow (CBF) in the MCA territory during the procedure (Fig. S2). After the occlusion period of 1 h, the monofilament suture was removed, followed by 24 h of reperfusion periods. The sham-operated mice were all treated similarly, except for MCAO. The whole operational procedure was conducted under the operating microscope. Mice were then placed into a temperature-controlled incubator for 4 h before returning to their home cages. All animals were allowed ad libitum access to water and food after surgery. Animals with brain hemorrhage, and those that did not show a reduction in CBF > 80% during MCAO and recovery of CBF > 70% after 5 min reperfusion, were excluded.

2.3. 2,3,5-Triphenyltetrazolium chloride (TTC) staining and infarct size assessment

Mice were anesthetized with chloral hydrate and sacrificed after 24 h reperfusion. The brains were quickly removed and chilled at −20 °C for 10 min and then, were sliced into 1-mm coronal sections. The brain slices were stained with 1% TTC at 37 °C for 5 min in dark and then fixed in 4% paraformaldehyde overnight. The unstained area of the brain slice was defined as infarction, whereas normal tissue was stained as red. Infarct volume ratio was measured and calculated. The healthy side brain area (A), ipsilateral non-infarcted brain regions (B) and infarct area (C) on both sides of the area were measured by Image-Pro Plus 5 image software. Infarct volume ratio (%) = (A-B) /A × 100%.

2.4. Modified neurological severity score

Modified neurological severity scores (mNSS) were used separately to grade various aspects on neurologic function after 24 h reperfusion. mNSS ranges from 0 to 14, in which 0 represents normal and 14 represents the highest degree of neurological deficiency. Neurologic severity score is composite of the motor, sensory, balance, and reflex tests. For the motor test, the bend and torsion of limbs were observed by holding up the tail of the mouse (0–3). The posture of walking on the floor was also assessed (0–3). For the balance test, the mice were placed on a beam. The neurological deficiency was assessed according to whether the mouse could keep balance on the beam, limbs fall off the beam, and walk through the beam (0–6). For the sensory and reflex tests, pinna and corneal reflex were examined, respectively (0–2). The higher the scores, the more severe is the injury.

2.5. Measurements of brain edema

To evaluate brain edema, brain water content was measured using the standard wet–dry method. After 24 h reperfusion, the brains were immediately removed. The two hemispheres were weighed (wet weight) separately, and then the tissue was dried at 100 °C for 24 h to determine the dry weight. The degree of brain edema was calculated using the following equation: water content = (wet weight–dry weight)/wet weight × 100%.

2.6. Immunohistochemistry

After 24 h or 72 h reperfusion, animals were perfused with 4% paraformaldehyde and brains then were dissected out and maintained in 4% paraformaldehyde overnight. They were transferred to 20% sucrose in phosphate-buffered saline (PBS) overnight and then to 30% sucrose overnight till the brains sunk to the bottom of the tube. Serial sections of the brains were cut (30-μm sections) using a vibrating microtome (Leica CM1950, Nussloch, Germany). Sections were incubated overnight with primary antibody against NeuN (1:800, Millipore, USA), GFAP (1:1000, Abcam, Cambridge, MA, USA) and Iba-1 (1:1000, AbD Serotec, Kidlington, UK), and then for 1 h with secondary antibodies. Immunoreactivity was visualized by incubation in substrate-chromogen solution (DAB). The total numbers of NeuN-positive neurons, GFAP-positive cells and Iba-1-positive cells were obtained stereologically using the Optical Fractionator method with Microbrightfield Stereo-Investigator software (Stereo Investigator software; Microbrightfield).

2.7. Primary astrocyte culture

Mouse primary astrocytes were prepared as described previously (Du et al., 2016). Briefly, neonatal mouse (P0–3) was sacrificed and then the cortices was removed and separated from meninges. Tissue was dissociated with 0.25% trypase (Amresco, Solon, OH) at 37 °C and terminated by Dulbecco's modified Eagle's medium (Gibco-BRL, Rockville, MD) supplemented with 10% fetal bovine serum (Sigma, St Louis, MO). After centrifugation at 1500 rpm for 5 min, the cell pellets were resuspended and plated on a poly-lysine–treated flask (Sigma, St Louis, MO). The cultures were maintained at 37 °C in a humidified 5% CO2–95% air atmosphere. Culture media were changed 24 h later to complete medium and subsequently twice a week. The purity of

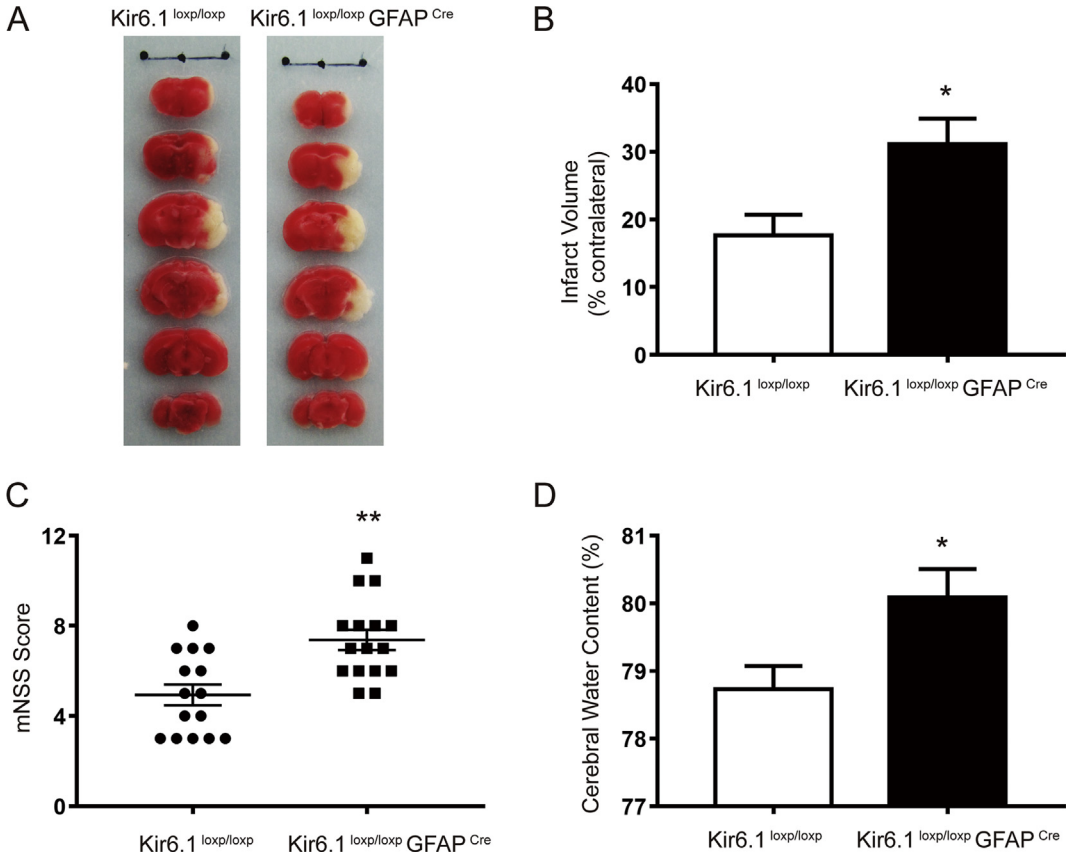

Fig. 1. Astrocytic Kir6.1 deletion increases infarct volume, neurological deficits, and brain edema in mice. A TTC staining of the brain slices from astrocytic Kir6.1 knockout (Kir6.1$^{loxp/loxp}$ GFAP^{Cre}) mice and WT (Kir6.1$^{loxp/loxp}$) mice in transient middle cerebral artery occlusion model. B The infarct volume was measured using the ImageJ analysis software (n = 5, Student's t-test). C Evaluation of the neurological deficits (n = 15–16, Mann–Whitney U test). D The brain water content (n = 5, Student's t-test). Values are expressed as mean ± SEM. $^{*}p < .05$, $^{**}p < .01$ vs Kir6.1$^{loxp/loxp}$ mice.

astrocyte was > 95% as determined with GFAP immunocytochemistry.

2.8. Cell transfection

Astrocytes at a confluency of 40–50% were transfected with small interfering RNA (siRNA) targeting Kir6.1 (Gene Pharma, Shanghai, China) using Lipofectamine™RNAi MAX (Thermafisher, USA) according to the instructions provided. A negative siRNA sequence was used as control (NC). After incubation for 6 h at 37 °C, the transfection mixture was removed and the cells were further incubated in complete growth media for 24 h. siRNA duplexes used were as follows: Kir6.1 sense: 5′-GCGACCAAUGUCAGGUCAUTT-3′; Kir6.1 antisense: 5′-AUGACCUG ACAUUGGUCACTT-3′; NC sense: 5′-UUCUCCGAACGUGUCACGUTT-3′; NC antisense: 5′- ACGUGACACGUUCGGAGAATT-3′.

2.9. Oxygen-glucose deprivation and reoxygenation (OGD/R) model

Oxygen-glucose deprivation and reoxygenation was performed as a model of ischemia/reperfusion (I/R) in vitro. For the OGD condition, the culture medium was replaced with glucose-free deoxygenatedcustom DMEM (GIBCO, CA, USA) and cells were maintained in a hypoxic chamber (Thermo scientific, Waltham, MA, USA) for 4 h with apremixed gas (1% O_2, 94% N_2, 5% CO_2). Reoxygenation was achieved by placing OGD-treated cells in glucose-containing DMEM under normoxic condition for 24 h (95% air and 5% CO_2). For non-OGD/R group, astrocytes were maintained in a complete DMEM medium and incubated in a normoxic conditions for 28 h.

2.10. Cell viability assay

Cell viability was evaluated using a 3-(4,5-dimethylthiazol-2-yl)-2,5-diphenyltetrazolium bromide (MTT) assay (R&D Systems Ltd., Europe) according to the manufacturer's instructions. The primary astrocytes were seeded in 96 well plates for 24 h. After OGD/R, 0.5 mg/mL MTT was added into the culture medium for 4 h. Then, the MTT solution was aspirated and dimethylsulfoxide (200 μL /well) was added. Optical density of the supernatant was read at 490 nm using a microplate spectrophotometer. Absorbances were normalized to the untreated control cultures which represented 100% viability. % Viability = Mean absorbance of sample/Mean absorbance of control ×100.

2.11. Flow cytometric apoptosis assay

Apoptosis rate was measured by flow cytometry using the AnnexinV-fluorescein isothiocyanate (FITC)/ propidium iodide (PI) apoptosis detection kit (BioVision, USA). Astrocytes were treated with 4-PBA (5 mM, TOCRIS, USA) for 1 h before OGD/R. Cold PBS was used to wash the obtained cells twice. Subsequently, the supernatant was discarded after centrifugation for 5 min at 1000 rpm. The pellets were resuspended with binding buffer. Cells were then mixed with Annexin V-FITC and PI, and the admixture was incubated for 10 min at room temperature according to manufacturer's protocol. Fluorescence signals were analyzed using a flow cytometer. Data were analyzed using the Cell Quest software (Guava Easy Cyte™8, Millipore, USA).

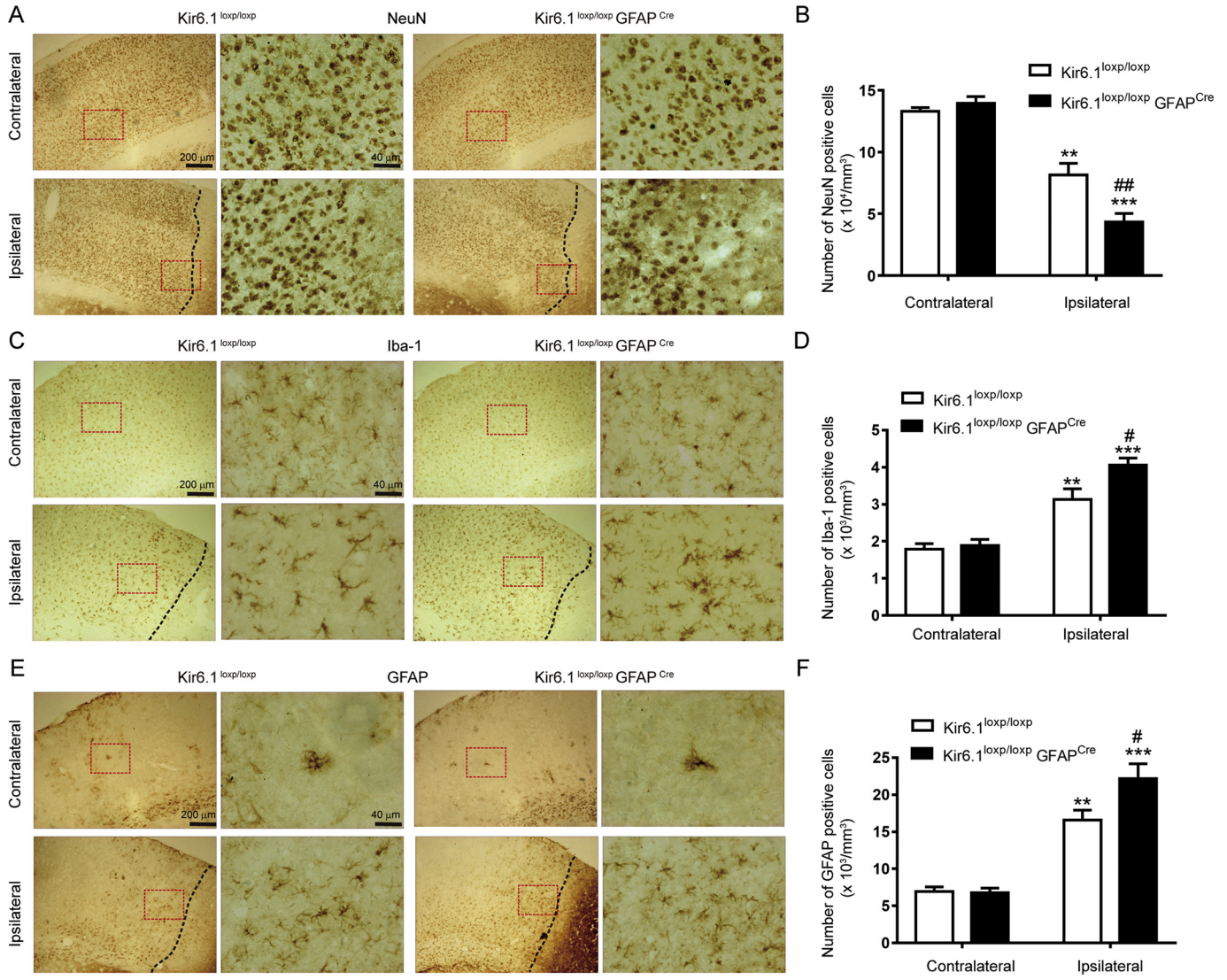

Fig. 2. Astrocytic Kir6.1 knockout exacerbates neuronal loss and glial activation after brain ischemic injury. A Neurons from cortex of infarct area were visualized by NeuN immunostaining in astrocytic Kir6.1 knockout (Kir6.1$^{loxp/loxp}$ GFAP^{Cre}) mice and WT (Kir6.1$^{loxp/loxp}$) mice at 24 h after transient middle cerebral artery occlusion (tMCAO). B Quantification of NeuN positive cells as shown in (A). C Activated microglia from cortex of infarct area were visualized by Iba-1 immunostaining at 24 h after tMCAO. D Quantification of Iba-1 positive cells as shown in (C). E Reactive astrocytes from cortex of infarct area were visualized by GFAP immunostaining at 72 h after tMCAO. F Quantification of GFAP positive cells as shown in (E). Values are expressed as mean ± SEM. n = 4–5, two-way ANOVA, $^{**}p < .01$, $^{***}p < .001$ vs corresponding contralateral; $^{\#}p < .05$, $^{\#\#}p < .01$ vs Kir6.1$^{loxp/loxp}$ mice ipsilateral.

2.12. Western blotting

Tissues and cell lysates were homogenized in lyses buffer (Beyotime, China) and protein concentration was determined by the Bradford assay (Bio-Rad, Hercules, CA, USA). The analysis of protein was performed according to standard SDS–PAGE. Immunoreactive bands were detected by enhanced chemiluminescence (ECL) plus detection reagent (Pierce, Rockford, IL) and analyzed using an Omega 16ic Chemiluminescence Imaging System (Ultra-Lum, Claremont, CA, USA). The following primary antibodies were used: primary antibody against CHOP (1:1000, CST, 2895, USA), GRP78 (1:1000, CST, 3183, USA), caspase-12 (1:800, CST, 2202, USA), β-actin (1:10000, CST, 3700, USA), BCL-2 (1:1000, CST, 2876, USA), BAX (1:1000, CST, 2772S, USA), caspase 3 (1:1000, CST, 9662, USA).

2.13. Statistical analysis

All data are expressed as means ± SEM. The differences with different treatments and genotypes were determined by two-way ANOVA, followed by the Tukey's post hoc test. Student's t-test was used to compare between two groups. Neurological scores were analyzed by Mann–Whitney U test. Statistical differences were considered significant when $p < .05$.

3. Results

3.1. Astrocytic Kir6.1 knockout increases infarct size, brain edema, and neurological deficits in tMCAO model mice

To study the function of the astrocytic Kir6.1/K-ATP channel in cerebral I/R injury, we established the tMCAO model with astrocytic Kir6.1 knockout (KO) mice and their control counterparts (WT). Consecutive TTC-stained coronal brain slices were arranged in cranial to caudal order (Fig. 1A). The white brain area represents infracted brain tissue. The astrocytic Kir6.1 KO mice exhibited larger infarct volume compared to WT mice (Fig. 1B). Also, the neurological deficits and brain edema were assessed 24 h after I/R injury. The neurological scores and brain water content in the astrocytic Kir6.1 KO mice were

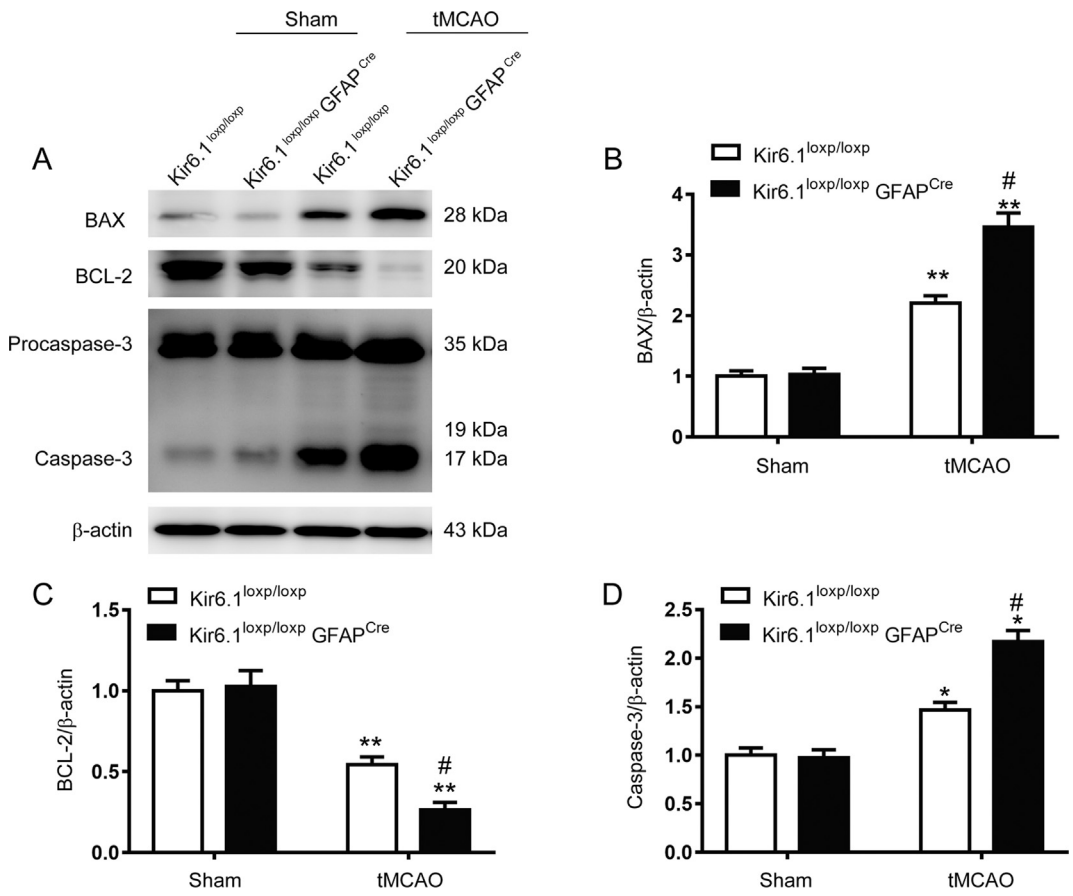

Fig. 3. Astrocytic Kir6.1 deletion promotes the expressions of apoptosis related proteins in the penumbra area during cerebral ischemia/reperfusion injury. A Representative immunoblots showing the expressions of apoptosis related proteins in the penumbra of astrocytic Kir6.1 knockout (Kir6.1$^{loxp/loxp}$ GFAP^{Cre}) mice and WT (Kir6.1$^{loxp/loxp}$) mice after transient middle cerebral artery occlusion (tMCAO). B-D Quantification of BAX (B), BCL2 (C) and caspase-3 (D) as shown in (A). Values are expressed as mean ± SEM. $n = 3$, two-way ANOVA, $^{*}p < .05$, $^{**}p < .01$ vs corresponding sham group; $^{\#}p < .05$ vs Kir6.1$^{loxp/loxp}$ mice tMCAO group.

significantly increased compared with those found in the WT mice (Fig. 1C, D). These results indicate that astrocytic Kir6.1 knockout aggravates cerebral I/R injury in mice.

3.2. Astrocytic Kir6.1 deletion exacerbates neuron loss and glial activation after cerebral I/R Injury

To further assess the role of astrocytic Kir6.1/K-ATP channel in the process of ischemic stroke, neuron survival and glial activation were measured by immunostaining with markers of neurons, astrocyte, and microglia in astrocytic Kir6.1 KO and WT mice after tMCAO. Significantly fewer NeuN positive neurons were detected in the brains of astrocytic Kir6.1 KO mice compared to that found in the WT mice (Fig. 2A, B, genotype: $p = .031$; MCAO: $p < .001$; interaction: $p = .005$), while more Iba1 positive microglia (Fig. 2C, D, genotype: $p = .018$; MCAO: $p < .001$; interaction: $p = .013$) and GFAP positive astrocytes (Fig. 2E, F, genotype: $p = .006$; MCAO: $p < .001$; interaction: $p = .015$) were detected in the brains of astrocytic Kir6.1 KO mice compared to those found in WT mice. Overall, these data suggest that astrocytic Kir6.1/K-ATP channel protects brain against cerebral ischemic injury.

3.3. Astrocytic Kir6.1 knockout promotes the expressions of apoptosis related proteins in the penumbra area during cerebral I/R injury

Apoptosis is a vital mode of cell death in the penumbra in acute and subacute period of ischemic stroke (Xia et al., 2018). BCL-2 and BAX belong to the BCL-2 protein family; BCL-2 promotes cell survival, whereas BAX accelerates apoptosis. Western blot analysis of brain tissues from the tMACO model showed that the expression of pro-apoptotic BAX protein was significantly increased in astrocytic Kir6.1 KO mice compared to that in WT mice (Fig. 3A, B, genotype: $p = .004$; MCAO: $p < .001$; interaction: $p = .010$), while, the expression of the anti-apoptotic protein BCL-2 was markedly reduced in astrocytic Kir6.1 KO mice compared to that in WT mice (Fig. 3A, C, genotype: $p = .004$; MCAO: $p < .001$; interaction: $p = .002$). More importantly, the level of cleaved-caspase-3, a specific effector for execution phases of apoptosis, was also significantly higher in astrocytic Kir6.1 KO mice than that in WT mice (Fig. 3A, D, genotype: $p = .010$; MCAO: $p < .001$; interaction: $p = .019$). These results suggest that astrocytic Kir6.1 knockout promotes I/R injury-induced apoptosis.

3.4. Astrocytic Kir6.1 deletion aggravates endoplasmic reticulum (ER) stress in the penumbra area during cerebral I/R injury

Increasing evidence indicates that ER stress is an initiator of cell death during hypoxia and I/R (Gulyaeva, 2015). To investigate the function of astrocytic Kir6.1/K-ATP channel in the regulating ER stress during cerebral I/R, the expressions of the ER stress biomarker, GRP78, and the ER stress-associated apoptotic markers, CHOP and cleaved caspase-12 were analyzed in the penumbra of astrocytic Kir6.1 KO and WT mice. As shown in Fig.4, the expressions of GRP78 (genotype: $p = .005$; MCAO: $p < .001$; interaction: $p = .004$), CHOP (genotype: $p = .036$; MCAO: $p < .001$; interaction: $p = .019$) and cleaved caspase-12 (genotype: $p = .004$; MCAO: $p < .001$; interaction: $p = .010$) were significantly increased in astrocytic Kir6.1 KO mice compared to those in WT mice. Together, these results suggest that astrocytic Kir6.1 knockout exacerbates ER stress response during cerebral I/R injury.

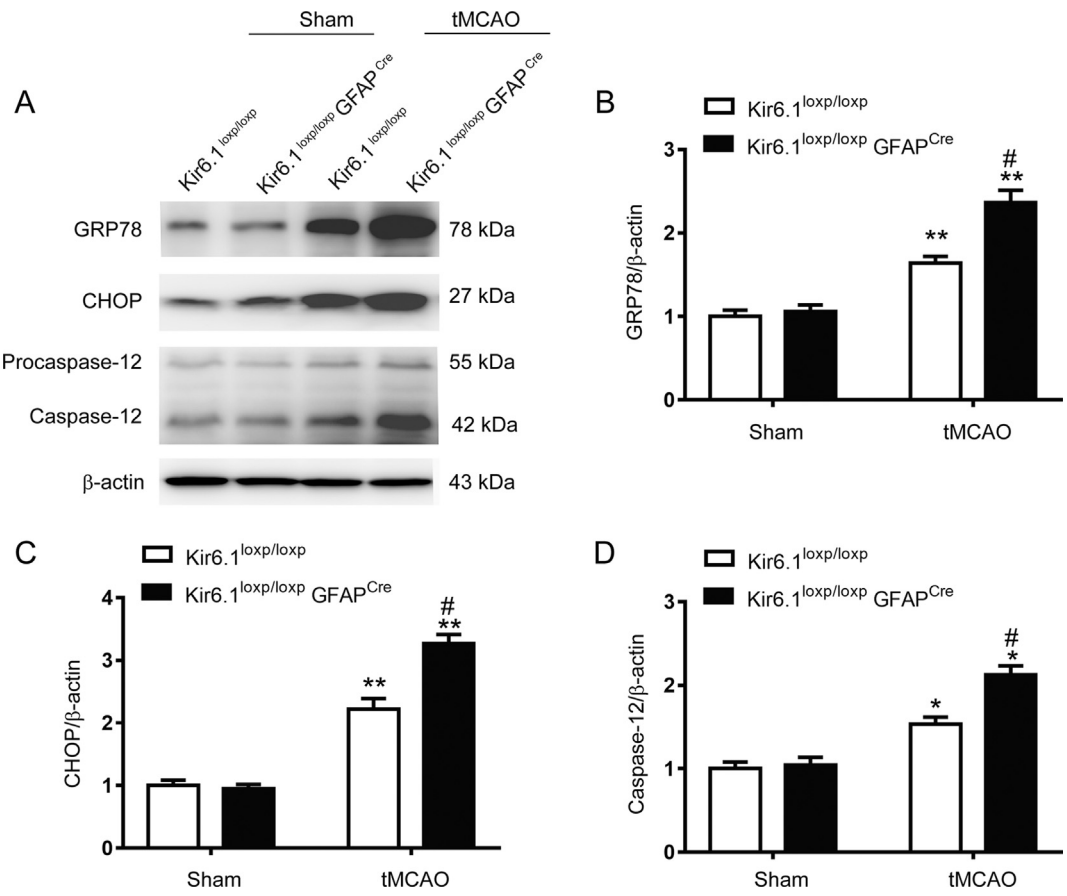

Fig. 4. Astrocytic Kir6.1 knockout aggravates endoplasmic reticulum (ER) stress in the penumbra area during cerebral ischemia/reperfusion injury. A Representative immunoblots showing overactivated ER stress in the penumbra of astrocytic Kir6.1 knockout (Kir6.1$^{loxp/loxp}$ GFAP^{Cre}) mice and WT (Kir6.1$^{loxp/loxp}$) mice after transient middle cerebral artery occlusion (tMCAO). B-D Quantification of GRP78 (B), CHOP (C) and caspase-12 (D) as shown in (A). Values are expressed as mean ± SEM. n = 3, two-way ANOVA, $^{*}p < .05$, $^{**}p < .01$ vs corresponding sham group; $^{\#}p < .05$ vs Kir6.1$^{loxp/loxp}$ mice tMCAO group.

3.5. Astrocytic Kir6.1 deficiency induces ER stress-associated apoptosis in primary cultured astrocytes during OGD/R injury

To test the impacts of astrocytic Kir6.1/K-ATP channel on astrocyte apoptosis, astrocytes transfected with Kir6.1 specific siRNA were subjected to the OGD/R procedure, followed by MTT and FACS analysis. MTT assay showed that knockdown of Kir6.1 significantly reduced cell viability of astrocytes in response to OGD/R treatment (Fig. 5A, genotype: $p = .037$; MCAO: $p < .001$; interaction: $p = .016$). As shown in Fig. 5B, cells appeared in the right upper and right lower quadrants of a dot plot represent all apoptotic cells. Compared to the negative control (NC) group, Kir6.1 knockdown group exhibited a much higher apoptotic rate (Fig. 5B, C, genotype: $p < .001$; MCAO: $p < .001$; interaction: $p < .001$). To confirm the involvement of ER stress in OGD/R-induced apoptosis, the protein levels of the ER stress biomarker, GRP78, and the ER stress-associated apoptotic markers, CHOP were analyzed under conditions of the normal and OGD/R treatment in astrocytes. The results indicated that the knockdown of Kir6.1 significantly increased the expressions of GRP78 (genotype: $p = .004$; MCAO: $p < .001$; interaction: $p = .003$) and CHOP (genotype: $p = .004$; MCAO: $p < .001$; interaction: $p = .003$) in OGD/R treated astrocytes compared to those in the case of NC group (Fig. 5D-F). These results demonstrate that astrocytic Kir6.1 knockout increases apoptosis and aggravates ER stress response in astrocytes during OGD/R injury.

3.6. Inhibiting ER stress reverses Kir6.1 knockout-induced apoptosis in primary cultured astrocytes during OGD/R injury

Our preceding data have strongly demonstrated that astrocytic Kir6.1 knockout promoted apoptosis and ER stress in astrocytes. To further determine whether Kir6.1 deletion derived ER stress contributes to cell apoptosis, we first pretreated astrocytes isolated from astrocytic Kir6.1 KO mice with ER stress inhibitor 4-PBA before OGD/R treatment. 4-PBA significantly increased cell viability of Kir6.1-deleted astrocytes (Fig. 6A). 4-PBA also reversed the increase in apoptotic rate due to Kir6.1 deletion (Fig. 6B, C). Furthermore, 4-PBA dramatically inhibited the expressions of BAX and cleaved-caspase-3 and increased the expression of BCL-2 in Kir6.1 knockout astrocytes (Fig. 6D-G). These results indicate that Kir6.1 knockout promotes apoptosis via ER stress-dependent pathway during OGD/R injury.

4. Discussion

Astrocytes are the most numerous cell types in the higher mammalian nervous system. They play key roles in modulate synaptic activity and structural, trophic, and metabolic support to neurons (Sims and Yew, 2017). Accordingly, impairment of astrocyte functions during brain ischemia and other insults are likely to influence neuronal survival and plasticity (Arbo et al., 2016). For decades, cerebral ischemia research was mainly focused on neuronal cells. It is a rather recent concept that astrocytes play significant roles in the demise of brain tissue after cerebral ischemia, in addition to protecting brain function and enhancing survival and regeneration under these conditions (Liu and Chopp, 2016). Therefore, subtle and temporal regulation of astrocyte functions after stroke will undoubtedly impact the survival of neurons (Becerra-Calixto and Cardona-Gomez, 2017). Kir6.1/K-ATP channel is mainly expressed in astrocytes (Thomzig et al., 2001). It has been found that Kir6.1 protein is present on hippocampal, cortical, and

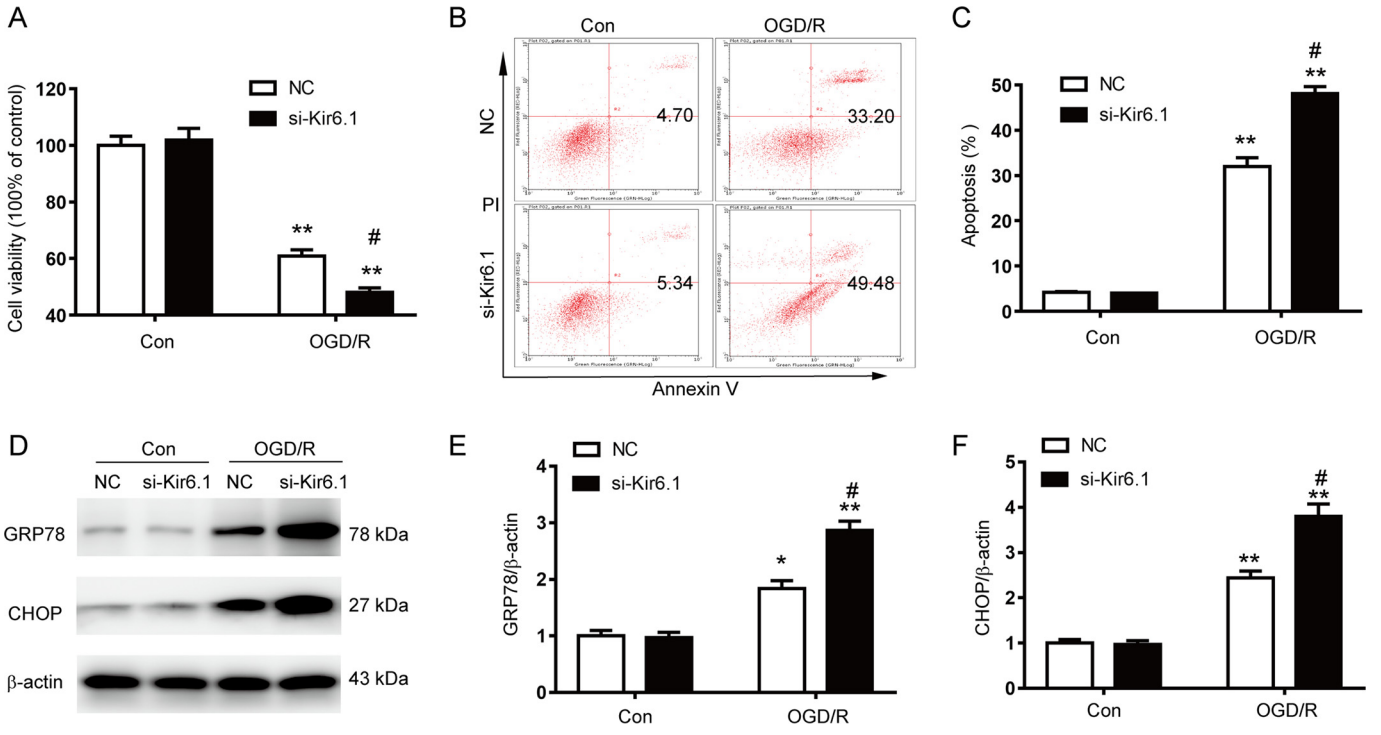

Fig. 5. Astrocytic Kir6.1 deficiency induces ER stress-associated apoptosis in astrocytes during oxygen-glucose deprivation and reoxygenation (OGD/R) injury. Astrocytes were transfected with negative control (NC) or specific Kir6.1 siRNA (si-Kir6.1) for 24 h, then exposed to OGD for 4 h and reoxygenation for 24 h (OGD/R), or maintained under normal conditions (Con). A Cell viability was detected by MTT assay. B Apoptosis was detected by flow cytometry with Annexin V-FITC/PI staining. C Quantification of apoptotic rates of astrocytes as shown in (B). D Representative immunoblots showing overactivated ER stress in astrocytes. E, F Quantification of GRP78 (E) and CHOP (F) as shown in (D). Values are expressed as mean ± SEM from three independent experiments, two-way ANOVA, $^{*}p < .05$, $^{**}p < .01$ vs corresponding control group; $^{\#}p < .05$ vs NC OGD/R group.

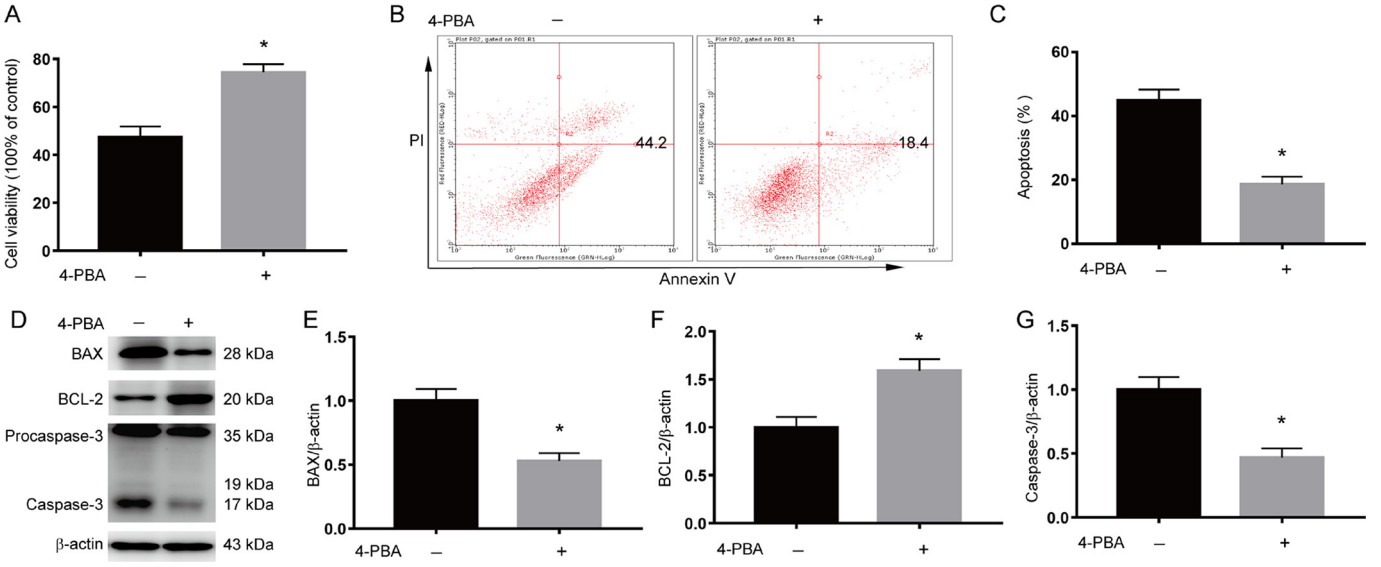

Fig. 6. Inhibition of ER stress reverses Kir6.1 knockout-induced apoptosis in astrocytes during oxygen-glucose deprivation and reoxygenation (OGD/R) injury. A Cell viability was detected by MTT assay in astrocytes isolated from astrocytic Kir6.1 knockout mice in the absence or presence of 4-PBA before OGD/R treatment. B Apoptosis was detected by flow cytometry with Annexin V-FITC/PI staining. C Quantification of apoptotic rates of astrocytes as shown in (B). D Representative immunoblots showing the expressions of apoptosis related proteins. *E*-G Quantification of BAX (E), BCL2 (F) and caspase-3 (G) as shown in (D). Values are expressed as mean ± SEM from three independent experiments, Student's t-test, $^{*}p < .05$.

cerebellar astrocytes, tanycytes, and Bergmann glial cells. Although Kir6.1, at the transcript level, appears to be highly expressed in human than mouse (Zhang et al., 2016a, b), the identification of Kir6.1 as the principal pore-forming subunit of plasma membrane K-ATP channels in astrocytes suggests that these glial K-ATP channels act in synergy with neuronal Kir6.2-mediated K-ATP channels during metabolic challenges in the brain. Our previous study showed that opening K-ATP channels could protect brain against ischemia injury via inhibition of inflammation (Dong et al., 2016). However, the exact role of astrocytic Kir6.1/K-ATP channel in ischemia stroke is unclear. In the present study, we showed that infarction volume (size) was significantly increased in astrocytic Kir6.1 KO mice compared to that in WT mice and

brain edema and neurological deficits were aggravated in astrocytic Kir6.1 KO mice. These results demonstrate that astrocyte-specific deletion of Kir6.1/K-ATP channel aggravates cerebral I/R injury in mice.

The ER stress is an essential step in the progression of brain I/R injury (Gulyaeva, 2015; Yang and Paschen, 2016). Certain stimuli such as ischemia, hypoxia, and hypertension might trigger the accumulation of unfolded proteins in the ER lumen, leading to the unfolded protein response (UPR) which involves expansion of ER membranes, accelerated degradation of unfolded proteins, increased translation of folding chaperones, and inhibition of other protein synthesis (Sanderson et al., 2015a). The UPR is initially a protective response aimed to restore ER functions predominantly through translational attenuation of proteins, up-regulation GRP78 and ER-associated degradation of unfolded proteins. If the stress is severe or prolonged, UPR can eventually result in promotion of pro-apoptotic pathways mediated by CCAAT/enhancer binding protein homologous protein (CHOP), caspase-12 and c-Jun N-terminal kinase (JNK) (Fu and Gao, 2014). It is possible that the timing of events for ER stress signaling regulation is important for the balance of life and death such that ER stress is initially protective, aiming to restore ER homeostasis, whereas prolonged *periods* of ER stress can be deleterious and damaging (Martin-Jimenez et al., 2017, Zhang et al., 2016a, b). Therefore, modulation of ER stress exerts a remarkable protective effect on the ischemic brain and offers the prospect of new stroke therapies (Sanderson et al., 2015b; Zhang et al., 2015). Here, we found that astrocytic Kir6.1 knockout exacerbated cell vulnerability to I/R injury and promoted astrocyte apoptosis. In addition, our results demonstrated that astrocytic Kir6.1 deletion significantly increased the expressions of GRP78, CHOP, and cleaved-caspase-12 in the peri infarct area following I/R injury and in astrocytes during OGD/R treatment. These findings suggest that astrocyte-specific deletion of Kir6.1/K-ATP channel aggravates cerebral ischemia/reperfusion injury through prolonged ER stress in mice and Kir6.1/K-ATP channel may be a key molecule in mediating ER stress in astrocytes.

Overwhelming evidence has suggested that in addition to necrosis, apoptosis also contributes significantly to cell death following cerebral I/R (Asadi et al., 2018). Recent studies have shown that ER stress is a critical component of the pro-apoptotic signaling pathway and in the sensing of brain injury after I/R (Wu et al., 2018; Gong et al., 2017). UPR activation can help reestablish homeostasis and normalize ER function, but if the injury is excessive, it can also lead to cell death (Nakka et al., 2016). ER stress also activates caspase-12, a member of the ICE (interleukin-1β converting enzyme) subfamily of caspases, which is localized to the ER and expressed at moderate levels in the brain (Wang et al., 2018). The active caspase-12 then activates subsequent caspases such as caspase-9 and caspase-3, induces DNA fragmentation and finally induces apoptosis (Martinez et al., 2010). In addition, CHOP is a transcription factor whose expression is upregulated during ER stress and it also participates in ER-mediated apoptosis. CHOP can further induce the expression of BAX and inhibit the expression of BCL-2 (Li et al., 2015). In this study, we demonstrated that astrocytic Kir6.1 knockout increased the protein levels of BAX and caspase-3, and decreased the BCL-2 level in vivo and in vitro. Furthermore, we found that 4-PBA, a potent ER stress inhibitor, markedly reversed the astrocytic Kir6.1 knockout-induced upregulation of BAX and caspase-3 and the number of cell apoptosis in astrocytes during OGD/R. These findings suggest that astrocytic Kir6.1/K-ATP channel is one of the crucial players in ER stress-associated apoptosis during I/R pathologic condition.

In conclusion, our findings demonstrate that astrocytic Kir6.1/K-ATP channel protects brain against cerebral ischemia/reperfusion injury via inhibiting excessive ER stress and suggest that astrocytic Kir6.1/K-ATP channel may be a promising therapeutic target for ischemia stroke.

Acknowledgements

This work was supported by the grants from the National Natural Science Foundation of China (81473195, 81630099 and 81473196) and Natural Science Foundation of Jiangsu Province (BK20151559).

Conflict of interest

The authors declare that they have no conflict of interest.

Appendix A. Supplementary data

Supplementary data to this article can be found online at https://doi.org/10.1016/j.expneurol.2018.10.005.

References

Arbo, B.D., Bennetti, F., Ribeiro, M.F., 2016. Astrocytes as a target for neuroprotection: Modulation by progesterone and dehydroepiandrosterone. Prog. Neurobiol. 144, 27–47.

Asadi, Y., Gorjipour, F., Behrouzifar, S., Vakili, A., 2018. Irisin Peptide Protects Brain against Ischemic Injury through reducing Apoptosis and Enhancing BDNF in a Rodent Model of Stroke. Neurochem. Res. https://doi.org/10.1007/s11064-018-2569-9.

Becerra-Calixto, A., Cardona-Gomez, G.P., 2017. The Role of Astrocytes in Neuroprotection after Brain Stroke: potential in Cell Therapy. Front. Mol. Neurosci. 10, 88.

Clarke, L.E., Liddelow, S.A., Chakraborty, C., et al., 2018. Normal aging induces A1-like astrocyte reactivity. Proc. Natl. Acad. Sci. U. S. A. 115, E1896–E1905.

Dong, Y.F., Wang, L.X., Huang, X., et al., 2013. Kir6.1 knockdown aggravates cerebral ischemia/reperfusion-induced neural injury in mice. CNS Neurosci Ther 19, 617–624.

Dong, Y.F., Chen, Z.Z., Zhao, Z., et al., 2016. Potential role of microRNA-7 in the anti-neuroinflammation effects of nicorandil in astrocytes induced by oxygen-glucose deprivation. J. Neuroinflammation 13, 60.

Du, R.H., Wu, F.F., Lu, M., et al., 2016. Uncoupling protein 2 modulation of the NLRP3 inflammasome in astrocytes and its implications in depression. Redox Biol. 9, 178–187.

Du, R.H., Sun, H.B., Hu, Z.L., et al., 2018. Kir6.1/K-ATP channel modulates microglia phenotypes: implication in Parkinson's disease. Cell Death Dis. 9, 404.

Fu, X.L., Gao, D.S., 2014. Endoplasmic reticulum proteins quality control and the unfolded protein response: the regulative mechanism of organisms against stress injuries. Biofactors 40, 569–585.

Ginsberg, M.D., 2008. Neuroprotection for ischemic stroke: past, present and future. Neuropharmacology 55, 363–389.

Gong, L., Tang, Y., An, R., et al., 2017. RTN1-C mediates cerebral ischemia/reperfusion injury via ER stress and mitochondria-associated apoptosis pathways. Cell Death Dis. 8, e3080.

Gulyaeva, N.V., 2015. Brain ischemia, endoplasmic reticulum stress, and astroglial activation: new insights. J. Neurochem. 132, 263–265.

Hirayama, Y., Ikeda-Matsuo, Y., Notomi, S., et al., 2015. Astrocyte-mediated ischemic tolerance. J. Neurosci. 35, 3794–3805.

Khakh, B.S., Sofroniew, M.V., 2015. Diversity of astrocyte functions and phenotypes in neural circuits. Nat. Neurosci. 18, 942–952.

Koizumi, S., Hirayama, Y., Morizawa, Y.M., 2018. New roles of reactive astrocytes in the brain; an organizer of cerebral ischemia. Neurochem. Int. https://doi.org/10.1016/j.neuint.2018.01.007.

Li, Y., Guo, Y., Tang, J., Jiang, J., Chen, Z., 2015. New insights into the roles of CHOP-induced apoptosis in ER stress. Acta Biochim. Biophys. Sin. Shanghai 47, 146–147.

Liddelow, S.A., Guttenplan, K.A., Clarke, L.E., et al., 2017. Neurotoxic reactive astrocytes are induced by activated microglia. Nature 541, 481–487.

Liu, Z., Chopp, M., 2016. Astrocytes, therapeutic targets for neuroprotection and neurorestoration in ischemic stroke. Prog. Neurobiol. 144, 103–120.

Maier, B., Gory, B., Taylor, G., et al., 2017. Mortality and Disability according to Baseline Blood pressure in Acute Ischemic Stroke patients Treated by Thrombectomy: a Collaborative Pooled Analysis. J. Am. Heart Assoc. 6. https://doi.org/10.1161/JAHA.117.006484.

Martinez, J.A., Zhang, Z., Svetlov, S.I., et al., 2010. Calpain and caspase processing of caspase-12 contribute to the ER stress-induced cell death pathway in differentiated PC12 cells. Apoptosis 15, 1480–1493.

Martin-Jimenez, C.A., Garcia-Vega, A., Cabezas, R., et al., 2017. Astrocytes and endoplasmic reticulum stress: a bridge between obesity and neurodegenerative diseases. Prog. Neurobiol. 158, 45–68.

Moussaddy, A., Demchuk, A.M., Hill, M.D., 2018. Thrombolytic therapies for ischemic stroke: Triumphs and future challenges. Neuropharmacology 134, 272–279.

Nakka, V.P., Prakash-Babu, P., Vemuganti, R., 2016. Crosstalk between Endoplasmic Reticulum stress, Oxidative stress, and Autophagy: potential Therapeutic Targets for Acute CNS Injuries. Mol. Neurobiol. 53, 532–544.

Rubaiy, H.N., 2016. The therapeutic agents that target ATP-sensitive potassium channels. Acta Pharma. 66, 23–34.

Sanderson, T.H., Gallaway, M., Kumar, R., 2015a. Unfolding the unfolded protein response: unique insights into brain ischemia. Int. J. Mol. Sci. 16, 7133–7142.

Sanderson, T.H., Gallaway, M., Kumar, R., 2015b. Unfolding the unfolded protein response: unique insights into brain ischemia. Int. J. Mol. Sci. 16, 7133–7142.
Sims, N.R., Yew, W.P., 2017. Reactive astrogliosis in stroke: Contributions of astrocytes to recovery of neurological function. Neurochem. Int. 107, 88–103.
Sun, H.S., Feng, Z.P., 2013. Neuroprotective role of ATP-sensitive potassium channels in cerebral ischemia. Acta Pharmacol. Sin. 34, 24–32.
Thomzig, A., Wenzel, M., Karschin, C., et al., 2001. Kir6.1 is the principal pore-forming subunit of astrocyte but not neuronal plasma membrane K-ATP channels. Mol. Cell. Neurosci. 18, 671–690.
Tinker, A., Aziz, Q., Thomas, A., 2014. The role of ATP-sensitive potassium channels in cellular function and protection in the cardiovascular system. Br. J. Pharmacol. 171, 12–23.
Wang, X., Shen, B., Sun, D., Cui, X., 2018. Aspirin ameliorates cerebral infarction through regulation of TLR4/NFkappaBmediated endoplasmic reticulum stress in mouse model. Mol. Med. Rep. 17, 479–487.
Wu, F., Qiu, J., Fan, Y., et al., 2018. Apelin-13 attenuates ER stress-mediated neuronal apoptosis by activating Galphai/Galphaq-CK2 signaling in ischemic stroke. Exp. Neurol. 302, 136–144.
Xia, Q., Li, X., Zhou, H., Zheng, L., Shi, J., 2018. S100A11 protects against neuronal cell apoptosis induced by cerebral ischemia via inhibiting the nuclear translocation of annexin A1. Cell Death Dis. 9, 657.
Yang, W., Paschen, W., 2016. Unfolded protein response in brain ischemia: a timely update. J. Cereb. Blood Flow Metab. 36, 2044–2050.
You, S., Saxena, A., Wang, X., et al., 2018. Efficacy and safety of intravenous recombinant tissue plasminogen activator in mild ischaemic stroke: a meta-analysis. Stroke Vasc Neurol 3, 22–27.
Yun, S.P., Kam, T.I., Panicker, N., et al., 2018. Block of A1 astrocyte conversion by microglia is neuroprotective in models of Parkinson's disease. Nat. Med. https://doi.org/10.1038/s41591-018-0051-5.
Zhang, H.Y., Wang, Z.G., Lu, X.H., et al., 2015. Endoplasmic reticulum stress: relevance and therapeutics in central nervous system diseases. Mol. Neurobiol. 51, 1343–1352.
Zhang, J., Chen, H., Huang, W., et al., 2016a. Unfolded protein response is activated in the ipsilateral thalamus following focal cerebral infarction in hypertensive rats. Clin. Exp. Pharmacol. Physiol. 43, 1216–1224.
Zhang, Y., Sloan, S.A., Clarke, L.E., et al., 2016b. Purification and Characterization of Progenitor and Mature Human Astrocytes reveals Transcriptional and Functional differences with Mouse. Neuron 89, 37–53.
Zhou, F., Yao, H.H., Wu, J.Y., et al., 2008. Opening of microglial K(ATP) channels inhibits rotenone-induced neuroinflammation. J. Cell. Mol. Med. 12, 1559–1570.
Zhou, Z., Lu, J., Liu, W.W., et al., 2018. Advances in stroke pharmacology. Pharmacol. Ther. https://doi.org/10.1016/j.pharmthera.2018.05.012.